DOI:10.22337/2587-9618-2025-21-4-56-72

DYNAMIC MODEL OF HIGH-FREQUENCY VIBRATION DAMPERS FOR POWER LINE CONDUCTORS

Alexander N. Danilin [1], Andrey P. Zakharov [2], Alexander E. Fedorov [1], Valery A. Feldstein [1,2]

[1] Institute of Applied Mechanics of the Russian Academy of Sciences, Moscow, RUSSIA
[2] Moscow Institute of Physics and Technology, Moscow, RUSSIA

Abstract: A dynamic model of an aeolian vibration damper for overhead power transmission line conductors has been developed, taking into account energy dissipation in the material structure. Based on the model, a dynamic stiffness matrix of the damper has been obtained, intended for use in a combined dynamic model of "conductor – damper". The damper's cable consoles are considered as beams made of a material with internal friction, to which the concept of microplastic deformations is applied. It is believed that the damper design is symmetrical relative to the vertical plane of the conductor sag, and during oscillations, it moves in this plane. The equations of oscillations are obtained in Lagrange form in matrix notations. The influence of the damping coefficient on energy dissipation power and oscillation amplitudes in resonance modes has been studied. The coefficients of amplitude and phase distribution (shape factor) of translational and rotational oscillations of loads have been determined depending on the radius of inertia and load eccentricity. Dimensionless nomograms of the damper arm's natural frequencies have been constructed in relevant parameter change ranges. The dependence of dimensionless dissipation power on frequency has been investigated.

Keywords: overhead power line, aeolian vibration, Stockbridge dampers, energy dissipation, dynamic model, dynamic stiffness matrix, parametric analysis, amplitude-frequency characteristics

ДИНАМИЧЕСКАЯ МОДЕЛЬ ГАСИТЕЛЕЙ ВЫСОКОЧАСТОТНЫХ ВИБРАЦИЙ ПРОВОДОВ ЛИНИЙ ЭЛЕКТРОПЕРЕДАЧИ

А.Н. Данилин [1], А.П. Захаров [2], А.Е. Фёдоров [1], В.А. Фельдштейн [1,2]

[1] Институт прикладной механики Российской академии наук, г. Москва, РОССИЯ
[2] Московский физико-технический институт, г. Москва, РОССИЯ

Аннотация: Разработана динамическая модель гасителя эоловой вибрации проводов воздушных линий электропередачи с учётом энергорассеяния в структуре материала. На основе модели получена матрица динамической жёсткости гасителя, предназначенная для использования в объединенной динамической модели «провод – гаситель». Тросовые консоли гасителя рассматриваются как балки из материала, обладающего внутренним трением, к которому применяется концепция микропластических деформаций. Считается, что конструкция гасителя симметрична относительно вертикальной плоскости провисания провода и при колебаниях она совершает движение в этой плоскости. Уравнения колебаний получены в форме Лагранжа в матричном виде. Исследовано влияние коэффициента демпфирования на мощность диссипации энергии и амплитуды колебаний в резонансных режимах. Определены коэффициенты распределения амплитуд и фаз-(коэффициент формы) поступательных и вращательных колебаний грузов в зависимости от радиуса инерции и эксцентриситета грузов. Построены безразмерные номограммы собственных частот плеча гасителя в актуальных диапазонах изменения параметров. Исследована зависимость безразмерной мощности диссипации от частоты.

Ключевые слова: воздушная линия электропередачи, эолова вибрация, гасители Стокбриджа, диссипация энергии, динамическая модель, матрица динамической жесткости, параметрический анализ, амплитудно-частотные характеристики

1. INTRODUCTION

The paper examines dynamic models of Stockbridge dampers utilized on overhead power lines (OHL) for the mitigation of aeolian vibrations, which arise from the intermittent release of Karman vortices from the conductor in wind flow [1]. Figure 1 depicts a frequently employed damper along with a schematic representation of its installation on a conductor [2].

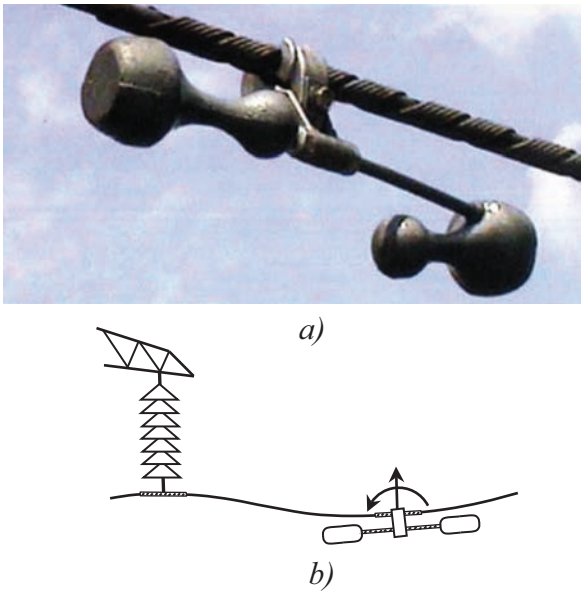

Figure 1. Vibration damper (a) and its installation diagram on the OHL conductor (b)

Mechanically, the damper consists of a pair of double arms (oscillators), with the inertial elements constructed as massive weights and the elastic elements designed according to traditional principles using elastic console cables. These cables also serve as dampers due to friction among the spiral wires that comprise them. In the presence of aeolian vibrations, a stationary transverse wave is established within the span, leading to kinematic excitation of the damper connected to the conductor. This excitation results in translational movement primarily in the vertical direction and rotation around an axis perpendicular to the plane of the conductor's sagging. Typically, the damper designs exhibit symmetry concerning the vertical plane of the conductor's sagging, and during oscillations, they perform planar motion within this plane.

The Stockbridge damper was developed in 1925 by George H. Stockbridge following several instances of damage to power transmission lines attributed to aeolian vibration [3]. Subsequently, the Stockbridge damper entered an extended phase of development and enhancement [3-7]. In 1932, R. Monroe and R. Templin proposed a two-degree-of-freedom damper.

Modern designs were developed as a result of extensive research conducted in the late 1960s and 1970s [6]. In 1968, R. Claren and G. Diana developed a variant of an asymmetric damper with various weights and arms of cable elements. A damper with two attachment points to a conductor, known as the Haro damper, was developed by L. Haro and T. Seppa in 1970. The Dogbone variant is another modern damper design that resembles a dog bone in shape. The damper was proposed by the Australian engineer and inventor Philip W. Dulhunty around 1976. The weights of the damper are slightly shifted to the side to create a third torsional degree of freedom, which allows the cable not only to bend vertically, but also to twist.

Despite the successful development of aeolian vibration dampers, practically no rules for designing dampers, analyzing their effectiveness and use were published at that time. Since the early 1970s, the first mathematical models of vibrations of Stockbridge dampers and similar variants began to appear [8-16]. H. Wagner et al. (1973) investigated the dynamic response of a symmetrical Stockbridge damper, which was modeled as a massless cable with weights attached to its ends [9]. P. Hagedorn (1980) proposed the concept of optimal the mechanical impedance of the damper, using a simple computational model [13]. The correctness of P. Hagedorn's approximate calculations was subsequently confirmed by B. Schaefer (1981) [15]. Based on these works, new design concepts for dampers with increased efficiency were considered [14].

In 1995, M. Markiewicz published a method and computational model for estimating the op-

timal dynamic characteristics of Stockbridge dampers designed for installation near anchor supports [16]. It is shown that the efficiency of a standard damper used in such spans can be increased due to its correct location on the conductor.

The bibliography of further research is extensive and covers various aspects of the vibrations of dampers themselves and the "conductor – dampers" systems. Significant results have been published, for example, in works [17-29].

In this paper, a dynamic vibration model of the damper is constructed, focused on further use in the combined dynamic model "conductor – damper". Such a combination is easily carried out if the dynamic stiffness matrix of the damper is known, which relates the amplitudes of the generalized forces applied to the clamp to the amplitudes of the generalized displacements caused by them. This article describes a dynamic model of the damper and a method for constructing the mentioned dynamic stiffness matrix, analyzes the spectrum of natural vibrations of the damper depending on the dimensionless values of the radius of inertia, the eccentricity of the weights and the damping coefficient. The dissipation in the elastic console is taken into account based on the model of internal friction, according to which the modulus of elasticity of the material is considered a complex quantity, the imaginary part of which characterizes the dissipation of vibration energy.

2. PHYSICAL MODEL AND VIBRATION EQUATIONS

The main function of a vibration damper is to dissipate mechanical energy due to friction and to change the shape of the conductor in the edge zone of the span in order to reduce bending deformations. In traditional Stockbridge type dampers with a console made of a cable, friction is provided by internal friction when the spiral wires that make up the cable slip. This allows consoles to be considered as beams made of a material with internal friction, to which the concept of microplastic deformations is applied [30, 31]. According to this model, the modulus of material elasticity is assumed to be complex: $E_K = E(1+i\eta)$, where η is the damping coefficient, which has the order of the logarithmic decrement of vibrations. Usually, due to the smallness of the internal friction, it is assumed that $\eta^2 << 1$. However, in this case, the damping is not assumed to be small. A refined version of relation is also known [31], which is used further:

$$E_K = E(a+ib),$$
$$a = \frac{1-\eta^2/4}{1+\eta^2/4}, \quad b = \frac{\eta}{1+\eta^2/4}. \tag{1}$$

Since $a^2+b^2=1$, then $a^2+b^2=1$, where $\psi = \operatorname{arctg}(b/a)$ and $E_\kappa = Ee^{i\psi}$. Therefore, taking into account the designation $D = EI$, the flexural rigidity of the console –

$$D_\kappa = E_\kappa I = EIe^{i\psi} = De^{i\psi}. \tag{2}$$

The primary mass of the damper is concentrated in the weights and the clamp; therefore, the inertia of the console is not taken into account.

The inertial elements of the damper – the clamp (along with the segment of conductor it encompasses) and the weights – are considered as rigid bodies characterized by their masses m_i, moments of inertia in the vertical plane $J_i = m_i r_i^2$ relative to their centers of mass C_i, and the distances (eccentricities) $|d_i| = P_i C_i$ between the centers of mass and the point designated as the pole. The indices $i = 0,1,2$ refer to the clamp, the left arm, and the right arm, as illustrated in figure 2.

Depending on the configuration of the weight, its center of mass C_i can be located on different sides of the attachment point P_i to the console. This option is used, for example, in VORTX™ vibration dampers by the well-known company

PLP (Preformed Line Products). This circumstance is taken into account by the sign of the eccentricity: $d_1 < 0$, $d_2 > 0$. Both possible attachment options for the weights are schematically shown in figure 1.2.

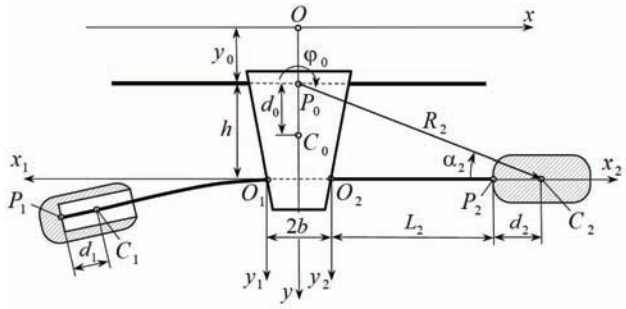

Figure 2. On deriving the vibration equations of the damper

It is assumed that the inertial characteristics of the loads, the lengths of the consoles L_i and the eccentricities d_i in the arms of the damper are different. This difference expands the frequency range of the damper and is used in practice.

The oscillations of the damper are considered with respect to a stationary right coordinate system $Oxyz$, the origin of which is located on the axis of the stationary conductor that is in equilibrium, and the longitudinal axis x is directed along the tangent. When aeolian vibration occurs, the clamp, along with the conductor, performs vertical and rotational oscillations relative to the axis Oz. Horizontal movements of the clamp can be neglected, as the longitudinal stiffness of the conductor is significantly greater than the transverse stiffness. The position of the clamp is determined by the vertical displacement y_0 of the point P_0 and the angle of rotation φ_0 relative to the stationary coordinate system. In addition to the stationary coordinate system, movable systems $O_i x_i y_i z_i \, (i = 1, 2)$ are introduced for each arm, which are associated with the clamp and therefore convenient for determining the deformations of the consoles.

As generalized coordinates for the clamp, the absolute coordinate y_0 and the angle of rotation φ_0 are chosen. It is advisable to choose the other generalized coordinates in such a way that the potential energy can be expressed as simply as possible in terms of the deflections and angles of rotation of the extreme sections of the console. This is convenient for further development of the model towards a more accurate account of the mechanical characteristics of the console, for example, to account for the dependence of the bending stiffness of the cables on their deflection [32]. For this purpose, movable coordinate systems $O_i x_i y_i z_i$ are used, relative to which the position of the weights is defined by the vertical displacements $y_{1,2}$ of the points $P_{1,2}$ and the angles of rotation $\varphi_{1,2}$. Then, the potential energy of the elastic deformations of the console takes the simplest form:

$$\Pi_i = \frac{1}{2}\left(g_i^{11} y_i^2 + 2 g_i^{12} y_i \varphi_i + g_i^{22} \varphi_i^2 \right),$$

where y_i, φ_i are deflection and angle of rotation at the extreme section of the console, and g_i^{mn} – elements of the stiffness matrix of the i-th console:

$$\boldsymbol{G}_i = \begin{pmatrix} 12 D_к / L_i^3 & -6 D_к / L_i^2 \\ -6 D_к / L_i^2 & 4 D_к / L_i \end{pmatrix}.$$

In the case under consideration

$$\Pi = \frac{1}{2} \sum_{i=1}^{2} \left(g_i^{11} y_i^2 + 2 g_i^{12} y_i \varphi_i + g_i^{22} \varphi_i^2 \right). \quad (3)$$

The total potential energy consists of the energy of elastic deformations of the console Π and the energy of the change in the center of gravity of the weights U. Let's evaluate these components. The inertia force of the weight, deforming the console, is of the order of $F = mA\omega^2$, where A – the amplitude of oscillations with frequency ω, and creates an average bending moment $M \approx mA\omega^2 L$ in the console, which corresponds

to the deformation energy Π: $M^2 L/D_K$. The gravitational part of the potential energy $U = mgA$. Comparing these values, we find: Π/U: $mA\omega^4 L^3/(D_K g)$. Even in the low-frequency range of aeolian vibration, at the amplitude $A \approx 0.01$м and typical parameters of the dampers [33], the elastic energy exceeds the gravitational energy by 1-2 orders of magnitude. It follows that the "pendulum" effect is insignificant for the operation of the system as an oscillation damper.

Kinetic energy of the damper:

$$K = \frac{m_0}{2}\left(V_0^2 + r_0^2\dot{\varphi}_0^2\right) + \frac{m_1}{2}\left[V_1^2 + r_1^2\left(\dot{\varphi}_0 - \dot{\varphi}_1\right)^2\right] + \\ + \frac{m_2}{2}\left[V_2^2 + r_2^2\left(\dot{\varphi}_0 + \dot{\varphi}_2\right)^2\right],$$

where V_i^2 are the squares of the absolute velocities of the centers of mass of the clamp $(i = 0)$ and weights $(i = 1,2)$, expressed in terms of their vertical and horizontal components:

$$V_0^2 = \dot{y}_0^2 + d_0^2\dot{\varphi}_0^2,$$
$$V_1^2 = \left(\dot{y}_0 + \dot{y}_1 + d_1\dot{\varphi}_1 - R_1\dot{\varphi}_0\cos\alpha_1\right)^2 + \\ + R_1^2\dot{\varphi}_0^2\sin^2\alpha_1,$$
$$V_2^2 = \left(\dot{y}_0 + \dot{y}_2 + d_2\dot{\varphi}_2 + R_2\dot{\varphi}_0\cos\alpha_2\right)^2 + \\ + R_2^2\dot{\varphi}_0^2\sin^2\alpha_2.$$

It is indicated here: $R_{1,2}^2 = \left(L_{1,2} + d_{1,2} + b\right)^2 + h^2$, and further it is taken into account that $R_{1,2}\cos\alpha_{1,2} = L_{1,2} + d_{1,2} + b = l_{1,2}$ (see figure 2).

The elementary work of the external forces applied to the clamp from the conductor side is equal to: $\delta A_y = F_C\delta y_0$, $\delta A_\varphi = M_C\delta\varphi_0$.

The equations of vibrations in the Lagrangian form [34, 35] can be presented in matrix notations. We will introduce a column vector of generalized coordinates and generalized external forces:

$$\boldsymbol{q} = \left(y_0\ \varphi_0\ y_1\ \varphi_1\ y_2\ \varphi_2\right)^T = \left(\boldsymbol{q}_0\ \boldsymbol{q}_1\ \boldsymbol{q}_2\right)^T, \\ \boldsymbol{Q} = \left(F_C\ M_C\ 0\ 0\ 0\ 0\right)^T, \tag{4}$$

as well as the inertia and stiffness matrices, which can be conveniently represented in block form:

$$\boldsymbol{M} = \begin{pmatrix} \boldsymbol{M}_{11} & \boldsymbol{M}_{12} & \boldsymbol{M}_{13} \\ \boldsymbol{M}_{12}^T & \boldsymbol{M}_{22} & \boldsymbol{0} \\ \boldsymbol{M}_{13}^T & \boldsymbol{0} & \boldsymbol{M}_{33} \end{pmatrix}, \\ \boldsymbol{C} = D_k\begin{pmatrix} \boldsymbol{0} & \boldsymbol{0} & \boldsymbol{0} \\ \boldsymbol{0} & \boldsymbol{C}_{22} & \boldsymbol{0} \\ \boldsymbol{0} & \boldsymbol{0} & \boldsymbol{C}_{33} \end{pmatrix}; \\ \boldsymbol{M}_{11} = \begin{pmatrix} m_\Sigma & \lambda_2 - \lambda_1 \\ \lambda_2 - \lambda_1 & \theta_\Sigma \end{pmatrix}, \\ \boldsymbol{M}_{22} = \begin{pmatrix} m_1 & \zeta_1 \\ \zeta_1 & \theta_1 \end{pmatrix},\ \boldsymbol{M}_{33} = \begin{pmatrix} m_2 & \zeta_2 \\ \zeta_2 & \theta_2 \end{pmatrix}, \\ \boldsymbol{M}_{12} = \begin{pmatrix} m_1 & \zeta_1 \\ -\lambda_1 & -\mu_1 \end{pmatrix},\ \boldsymbol{M}_{13} = \begin{pmatrix} m_2 & \zeta_2 \\ \lambda_2 & \mu_2 \end{pmatrix}, \tag{5}$$

where:

$$m_\Sigma = m_0 + m_1 + m_2,$$
$$\theta_\Sigma = m_0(r_0^2 + d_0^2) + m_1(R_1^2 + r_1^2) + m_2(R_2^2 + r_2^2)$$

– mass and moment of inertia of the entire damper relative to the pole O; $\theta_i = m_i(r_i^2 + d_i^2)$ – moments of inertia of weights relative to the poles P_i; $\zeta_i = m_i d_i$, $\lambda_i = m_i l_i$, $\mu_i = m_i(r_i^2 + d_i l_i)$ $(i = 1,2)$; $\boldsymbol{C}_{22} = \boldsymbol{G}_1$, $\boldsymbol{C}_{33} = \boldsymbol{G}_2$; $\boldsymbol{0}$ – zero 2×2-matrix.

Then the equations of vibrations will be written in the form:

$$\boldsymbol{M}\ddot{\boldsymbol{q}} + \boldsymbol{C}\boldsymbol{q} = \boldsymbol{Q}. \tag{6}$$

The forced vibrations of the damper installed on the vibrating conductor in the OHL span (span mode) [36] are excited by the action of periodic force and moment from the conductor, so that

the vector of generalized forces in the right part of (6) has the form

$$\boldsymbol{Q} = \left(F_C e^{i\omega t} \;\; M_C e^{i\omega t} \;\; 0 \;\; 0 \;\; 0 \;\; 0 \right)^T . \qquad (7)$$

This mode is further considered when determining the dynamic stiffness matrix used in constructing the combined "conductor – damper" model.

Important characteristics of vibration dampers include natural frequencies, amplitude-frequency characteristics (AFC), and the power of mechanical energy dissipation performed by the damping element of the damper. Current regulatory documents, for example [36], provide for its experimental determination through tests on a vibration stand that implements harmonic oscillations of the platform with an amplitude that changes according to the law $A(\omega)$.

In this case, the damper clamp is fixed immovably on the stand platform, while the weights perform a complex motion: a translational motion together with the stand platform and a relative motion with respect to the platform (stand mode). Then the loads are affected by the inertia of the portable motion, which reduces to a force and a moment with amplitudes $m_i A\omega^2$ and $d_i m_i A\omega^2$, as follows from (5), at $y_0 = Ae^{i\omega t}$, $\varphi_0 = 0$.

Therefore, in relation to this mode, in the general equation (6), the vector $\boldsymbol{q}$ defines the relative motion, and the vector $\boldsymbol{Q}$ defines the portable inertia forces. When testing the dampers, the frequency amplitude is scanned in such a way that the set amplitude of the platform speed is maintained $A\omega = V = (0.05 - 0.2)\,\text{m/s}$, so that

$$\boldsymbol{Q} = \left(0 \;\; 0 \;\; m_1\omega V \;\; d_1 m_1 \omega V \;\; m_2 \omega V \;\; d_2 m_2 \omega V \right)^T .$$

In the experiments, the damper arms oscillate practically independently; the weak mutual influence due to the elasticity of the clamp should be attributed to nonlinear effects that are insignificant in this case and is not taken into account. Such independent – partial oscillations of individual arms are also of interest and are described by equation (6), if instead of the general matrices $\boldsymbol{A}$, $\boldsymbol{C}$, we use their blocks A_{22}, C_{22}, or , A_{33}, C_{33}:

$$\begin{aligned} \left(C_{22} - \omega^2 M_{22} \right) \boldsymbol{q}_1 &= \boldsymbol{Q}_1 , \\ \left(C_{33} - \omega^2 M_{33} \right) \boldsymbol{q}_2 &= \boldsymbol{Q}_2 . \end{aligned} \qquad (8)$$

2. DYNAMIC CHARACTERISTICS OF THE DAMPER

In the following, we will focus on the design parameters that are typical for practically used vibration dampers (see table 1).

Table 1. Parameters of a typical vibration damper

Weight		
Mass m, kg	Radius of inertia r, mm	Eccentricity d, mm
1	40	15
Console		
Bending stiffness D, $\text{N}\cdot\text{m}^2$	Length L, mm	
1–6	100	
Clamp		
Mass m_0, kg	Moment of inertia J_0, $\text{kg}\cdot\text{m}^2$	
0.3	0.0003	

Setting the bending stiffness in the form of a range is due to the fact that this parameter for a console made of a spiral cable depends on the amplitude of the weight vibrations. At low amplitudes, the individual wires are pressed against each other and the console deforms like a solid section beam; in this case, the stiffness has the maximum value $D \approx 6\ \text{Н}\cdot\text{м}^2$. At high amplitudes, the wires slip each other in the console, as a result of which each of them bends independently; as a result, the stiffness of the console decreases and reaches a minimum value

$D \approx 1\ \text{Н}\cdot\text{м}^2$. This means that the elastic element in the form of a spiral cable, generally speaking, has a non-linearity.

Partial oscillations realized in the stand mode are described by equations (8). Due to the identity of the equations, the subscripts will be omitted when considering a single equation. Let us write down the system of equations with respect to the oscillation amplitudes in an expanded form, assuming: $y = Ye^{i\omega t}$, $\varphi = \Phi e^{i\omega t}$:

$$\begin{pmatrix} g^{11} - m\omega^2 & g^{12} - \varsigma\omega^2 \\ g^{12} - \varsigma\omega^2 & g^{22} - \theta\omega^2 \end{pmatrix} \begin{pmatrix} Y \\ \Phi \end{pmatrix} = \omega V \begin{pmatrix} m \\ \varsigma \end{pmatrix}. \quad (9)$$

In the following, the notation is used:

$$\rho = r/L,\ \delta = d/L,\ f = Y/L,$$
$$p = \omega\sqrt{mL^3/3D} = \omega/\omega_0,$$

where ω_0 is the lowest natural frequency of the console with bending stiffness and point mass m at the free end of the console. Turning to these variables, we transform the system (9) to the form

$$\begin{pmatrix} 4e^{i\psi} - p^2 & -2e^{i\psi} - \delta p^2 \\ -2e^{i\psi} - \delta p^2 & 4e^{i\psi}/3 - (\delta^2 + \rho^2)p^2 \end{pmatrix} \begin{pmatrix} f \\ \Phi \end{pmatrix} = \frac{Vp}{L\omega_0} \begin{pmatrix} 1 \\ \delta \end{pmatrix}. \quad (10)$$

Considering (1), (2), the solution of these equations is written as:

$$f = \frac{V}{L\omega_0}\frac{p}{\Delta}\left[2e^{i\psi}\left(\frac{2}{3} + \delta\right) - \rho^2 p^2\right] = \frac{V}{L\omega_0} f_*,$$
$$\Phi = \frac{V}{L\omega_0}\frac{p}{\Delta} 2e^{i\psi}\left(1 + 2\delta\right) = \frac{V}{L\omega_0}\Phi_*. \quad (11)$$

Here:

$$\Delta(p) = \rho^2 p^4 - 4p^2 e^{i\psi} c + 4e^{2i\psi}/3 = \Delta_R + i\Delta_I$$

is the determinant of the system (10); dimensionless variables:

$$\Delta_R = \rho^2 p^4 - 4p^2 ca + 4\left(a^2 - b^2\right)/3,$$
$$\Delta_I = 4b\left(2a - p^2 c\right);$$
$$f_* = \frac{p}{\Delta_R^2 + \Delta_I^2}(f_R + if_I)(\Delta_R - i\Delta_I), \quad (12)$$
$$\Phi_* = \frac{p}{\Delta_R^2 + \Delta_I^2} 2(1 + 2\delta)(a + ib)(\Delta_R - i\Delta_I),$$

with coefficients:

$$c = 1/3 + \rho^2 + \delta(\delta + 1),$$
$$f_R = 2a(2/3 + \delta) - \rho^2 p^4,\ f_I = 2b(2/3 + \delta). \quad (13)$$

The ratio of amplitudes during frequency scanning varies according to the law:

$$\beta = \frac{\Phi_*}{f_*} = \frac{2\left(1 + 2\delta\right)}{f_R^2 + f_I^2}(\beta_R + i\beta_I), \quad (14)$$

where are the real and imaginary parts:

$$\beta_R = af_R + bf_I,\ \beta_I = bf_R - af_I. \quad (15)$$

Let's first consider the characteristics of the damper without taking into account damping. The equation $\text{Re}\left[\Delta(p)\right] = 0$ defines the natural frequencies of free harmonic oscillations of a conservative system. In the expanded form –

$$\left(3\rho^2/4\right)p^4 - 3cp^2 + 1 = 0 \quad (16)$$

with discriminant $\vartheta(\delta, \rho) = 9c^2 - 3\rho^2 \geq 0$.

It is fundamentally important that the natural frequencies of the damper are located in the current frequency range characteristic of aeolian vibration. As can be seen, the dimensionless partial frequencies of the damper are determined by two parameters δ and ρ, moreover, a pair of values $\delta = -1/2$, $\rho = 1/\sqrt{12} = 0,289$ (solu-

tion of the system of equations $\partial\vartheta/\partial\delta = 0$, $\partial\vartheta/\partial\rho = 0$) plays a special role: for these values, the discriminant of equation (16) is zero and its roots are multiples. In dimensional variables, this means that when $d = -\sqrt{3}\,r$ both frequencies coincide: $\omega_1 = \omega_2 = \sqrt{12D/mL^3}$.

Figure 3 shows the dependences of the dimensionless frequencies $p_{1,2}$ on the eccentricity of the load (parameter δ) at different values of the radius of inertia (parameter ρ).

The curves corresponding to $\delta = -1/2$, $\rho = 1/\sqrt{12} \approx 0.289$ are limiting: at $\delta \to -1/2$, the frequencies approach each other: the lower frequency p_1 reaches its maximum, and the upper frequency p_2 reaches its minimum, and $p_1(-1/2) = p_2(-1/2) = 2$.

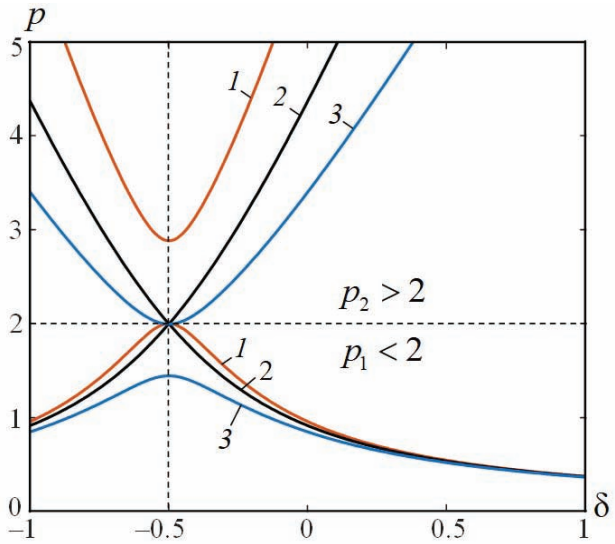

Figure 3. Dependencies $p_{1,2}(\delta)$ for different parameter values $\rho = 0.2,\ 0.289,\ 0.4$ (curves 1, 2, 3, respectively)

The symmetry of the curves relative to the vertical $\delta = -1/2$ shows that from the point of view of controlling the natural frequencies by choosing the geometry of the damper, the schemes at $|\delta| > 1/2$ are irrational. For designing a low-frequency damper for damping vibration, for example, in the band ≈ 5 Hz and below, a scheme in which both frequencies lie in a narrow low-frequency region may be rational. The proximity of the frequencies is achieved by purely geometric means: negative eccentricity and mass distribution, and the "smallness" of the frequencies is achieved by choosing the parameters that determine the scale frequency $\omega_0 = \sqrt{3D/mL^3}$.

From the point of view of practical properties of the damper, designs with multiple frequencies should be considered irrational for the following reasons. Firstly, instead of two frequencies at which the damping effect is manifested, there remains one, which narrows the operating frequency range of the device. Secondly, transverse and torsional vibrations are realized independently, i.e. there is no connection between them, which leads to a decrease in the damping efficiency. In this regard, it is possible not to consider variants with a strong negative eccentricity, when $\delta < -1/2$. The proximity of $\delta \approx -1/2$ is also inappropriate, since in this case the amplitude distribution coefficients (shape factor) and phase relationships of translational and torsional vibrations of loads, determined from the first equation (10) at $\psi = 0$, reveal a strong dependence on the geometric parameters δ and ρ:

$$\gamma_{1,2} = \frac{\Phi_{1,2}}{f_{1,2}} = \frac{4 - p_{1,2}^2(\delta,\rho)}{2 + \delta \cdot p_{1,2}^2(\delta,\rho)}. \qquad (17)$$

Note the difference between relations (14) and (17). The first relates to forced oscillations and is a function of the excitation frequency; the second relates to free oscillations at natural frequencies. Of course, at natural frequencies in the absence of damping they coincide: $\gamma_{1,2} = \beta_{1,2}$.

The signs of the quantities $\gamma_{1,2}$ determine the relationship of the oscillation phases. With a positive eccentricity $(\delta > 0)$, the denominator is positive and the sign of the coefficients $\gamma_{1,2}$ depends only on the frequency. As follows

from the graphs in figure 3 $p_1 < 2$, $p_2 > 2$. Therefore, at the first natural frequency, the generalized coordinates change in phase, and at the second, they are in antiphase, regardless of the parameters δ, ρ and, therefore, the geometry of the weights. However, with a negative eccentricity $(\delta < 0)$, the signs and values of the shape factors depend in a complex way on the relationship of the geometric parameters δ, ρ, as evidenced by the curves in figure 4. In practical terms, such a strong dependence can manifest itself in instability of the oscillation modes.

Taking into account the above, nomograms of the natural frequencies of the damper arm in the current ranges of change of the eccentricity (ρ) and the radius of gyration of the load (δ) are calculated (figure 5). The given dependencies can be used for rational "tuning" of the damper to the required frequency range.

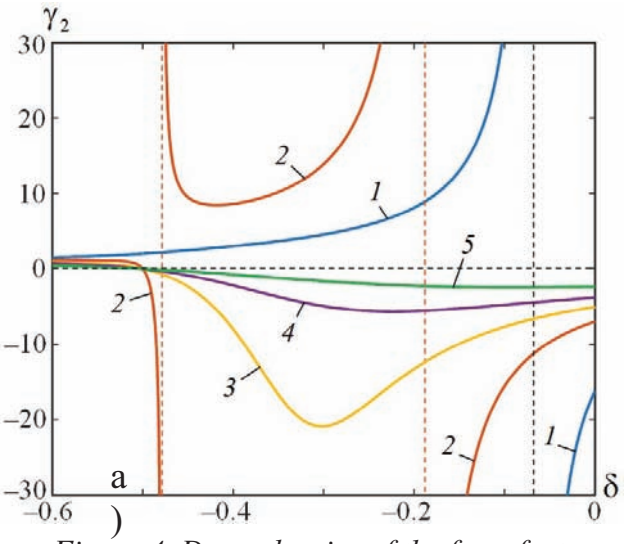

Figure 4. Dependencies of the form factor $\gamma_2(\delta)$ *for different values of the parameter* $\rho = 0.2, 0.3, 0.35, 0.4, 0.5$ *(curves 1–5)*

With small damping, the natural frequencies practically coincide with the resonant frequencies of the real system. However, in the case of a damper, the function of which is to dampen oscillations, it is advisable to make the attenuation sufficiently large, which can lead to a divergence of the natural and resonant frequencies.

The latter are revealed in the amplitude-frequency characteristics, determined experimentally during tests on a vibration stand or theoretically from the solution of non-homogeneous equations. Since the conditions for excitation of forced oscillations can be different, the AFC also differ. Of practical importance are the conditions of the stand and the conditions of the flight, that is, excitation from the side of the wire on which the damper is installed.

Let us consider a variant of an equal-shoulder damper under stand conditions, returning to equations (10) and their solution (11). In accordance with formulas (12), expressions for modules of functions $\left|f(p)\right|$, $\left|\Phi(p)\right|$ have the form:

$$\left|f(p)\right| = p\sqrt{\frac{f_R^2 + f_I^2}{\Delta_R^2 + \Delta_I^2}},$$
$$\left|\Phi(p)\right| = p\frac{2(1+2\delta)}{\sqrt{\Delta_R^2 + \Delta_I^2}}. \qquad (18)$$

Formulas (18) represent the AFC of the damper under stand conditions. They are graphically shown in figure 6 a) and b). The calculations were performed using the values of the parameters: $\eta = 0.1...0.5$, $\rho = 0.4$, $\delta = 0.15$.

The graphs of the functions $\left|f(p)\right|$, $\left|\Phi(p)\right|$ show that in this case damping plays a significant role only at resonances; at intermediate frequencies, the calculation results with and without internal friction are almost identical. The resonant frequencies of the damped and conservative systems (the latter are equal in this case $p_1 = 0.72$, $p_2 = 4.02$) also practically coincide.

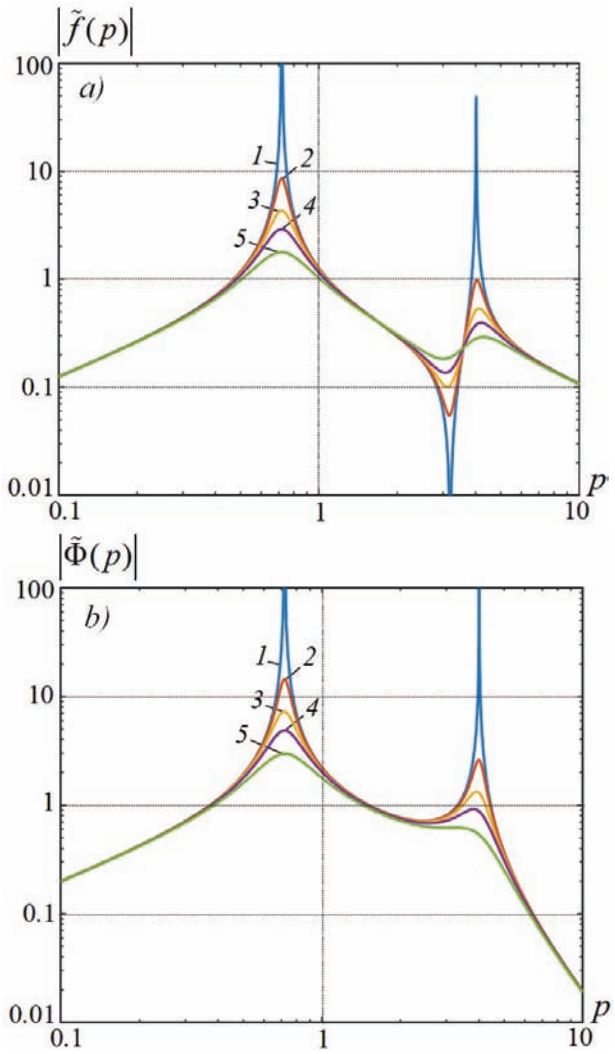

Figure 6. AFC of the damper at different values of the damping coefficient (curves 1–5)

Note that, as follows from (11), at $p \approx \sqrt{4/3+2\delta}/\rho$, the amplitude of vertical vibrations of the load drops sharply (in the absence of friction, it turns to zero). This is a manifestation of the Den Hartog effect [37], when, during forced oscillations of a system with two degrees of freedom at a certain frequency, one of the generalized coordinates "freezes", which is used to dampen vibrations. This effect is clearly manifested in the absence of friction (the first curve in figure 6 a), however, in relation to the damper, it is rather a negative factor. Note also that the dimensionless AFC $|\tilde{f}(p)|$, $|\tilde{\Phi}(p)|$ do not depend on the frequency scanning mode, which appears only when returning to the dimensional values according to (11).

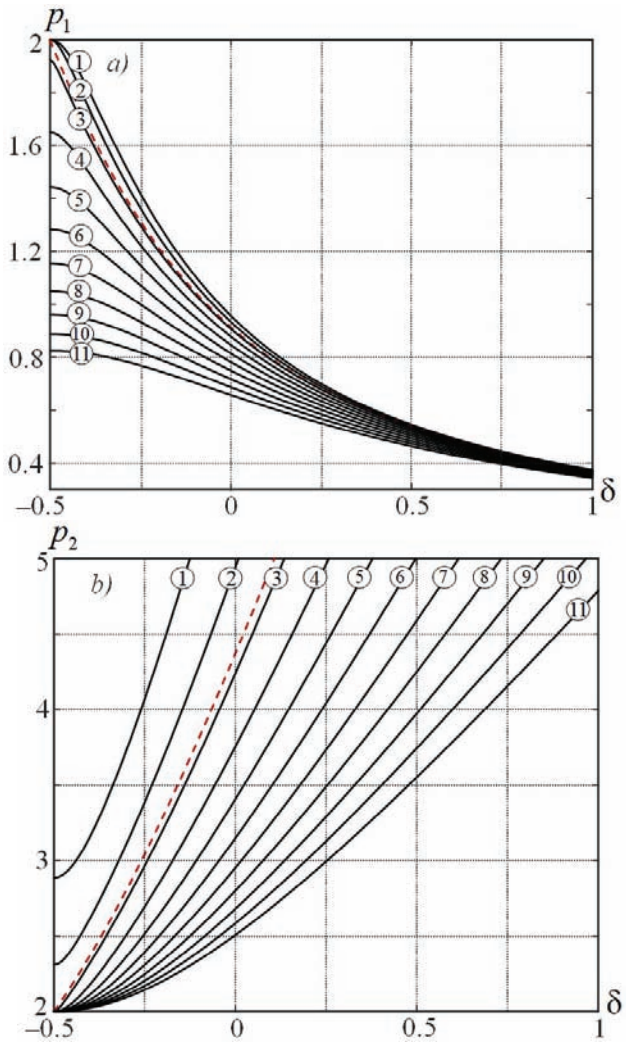

Figure 5. Dependences of the dimensionless natural frequencies of the damper arm $p_{1,2}(\delta)$ at $\rho = 0.2 - 1.2$ (curves 1–11 in increments 0.1); the dotted line shows the dependences at the "boundary" value $\rho = 0.289$

Next, we consider the frequency dependence of dissipation on the frequency of forced oscillations. The power dissipation of mechanical energy due to internal friction in each arm of the damper, as follows from (3), is equal to the imaginary part of the amplitude value of the potential energy divided by a quarter of the oscillation period:

$$W = \frac{12D\omega}{\pi L}\left| f^2 - f\Phi + \frac{1}{3}\Phi^2 \right| \sin\psi \,.$$

Considering (11) and the relation (14) between the amplitudes of translational and rotational oscillations, we find:

$$W = mV^2\omega_0\Theta\left(\delta,\rho,\psi,p\right),$$

where

$$\Theta\left(\delta,\rho,\psi,p\right) = \frac{4}{\pi}p\left|f^2\right|\left|1-\beta+\frac{1}{3}\beta^2\right|\sin\psi \quad (19)$$

is a dimensionless function of only the dimensionless geometric parameters of the damper, the damping coefficient in the form (2) and the frequency. Using (12)-(15), it is not difficult to obtain expressions for modules:

$$\left|f^2\right| = p^2\frac{f_R^2+f_I^2}{\Delta_R^2+\Delta_I^2},$$

$$\left|1-\beta+\frac{1}{3}\beta^2\right| = \frac{1}{f_R^2+f_I^2}\sqrt{\Theta_R^2+\Theta_I^2},$$

where

$$\Theta_R = f_R^2 + f_I^2 -$$

$$-2(1+2\delta)\left[\beta_R - \frac{2}{3}\frac{1+2\delta}{f_R^2+f_I^2}\left(\beta_R^2-\beta_I^2\right)\right],$$

$$\Theta_I = -2(1+2\delta)\beta_I\left[1-\frac{4}{3}\frac{1+2\delta}{f_R^2+f_I^2}\beta_R\right].$$

Then, instead of (19), we will have the formula:

$$\Theta\left(\delta,\rho,\psi,p\right) = \\ = \frac{4}{\pi}\frac{p^3}{\Delta_R^2+\Delta_I^2}\sqrt{\Theta_R^2+\Theta_I^2}\sin\psi\,. \quad (20)$$

Figure 7 shows the dependences of the dimensionless dissipation power (20) on the frequency p at values $\eta = 0.1,\ 0.5$.

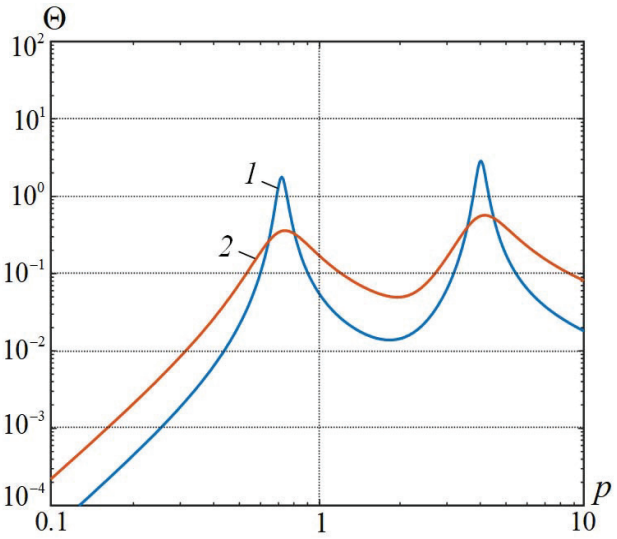

Figure 7. Dependence of the dimensionless dissipation power on the frequency at values $\eta = 0.1,\ 0.5$ *(curves 1, 2);* $\rho = 0.4,\ \delta = 0.15$

Note that as the damping coefficient increases, the dissipation power at the resonances decreases, while away from the resonances, on the contrary, it increases. At first glance, this strange phenomenon is explained by the fact that as η increases, the resonant amplitude of oscillations a decreases For example, for a single-degree oscillator with internal friction, excited by a vibration stand with a table amplitude A, it is inversely proportional to η: $a \sim A/\eta$. At the same time, the power of dissipation $w \sim a^2\eta$. It follows that $w \sim A^2/\eta$. A similar result holds for an oscillator with viscous Rayleigh friction. In the practice of designing and testing dampers, it is known that the dissipation power is reduced by artificially increasing damping by increasing interwire friction, which led to the "locking" of the cable console.

In a system with two degrees of freedom, the situation is different. Figure 8 shows the dependences of the dissipation power at the damper resonances on the damping coefficient (solid curves).

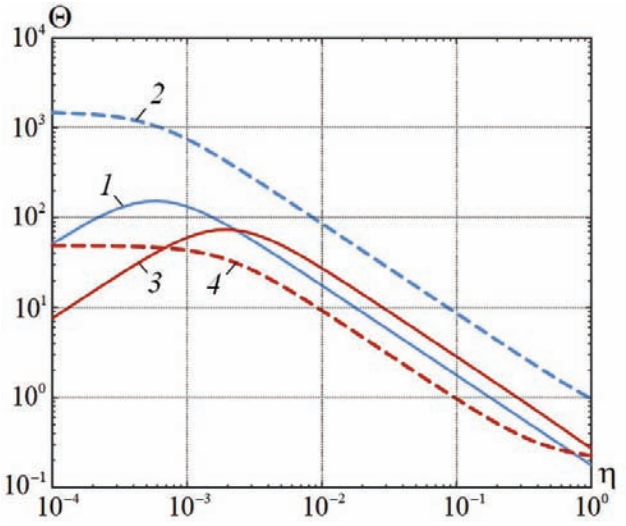

Figure 8. The influence of the damping coefficient on the dimensionless dissipation power (solid curves 1, 3) and the amplitude of vertical oscillations (dashed curves 2, 4) in resonant modes at $p_r = 0.719$ *(curves 1, 2) and* $p_r = 4.02$ *(curves 3, 4);* $\rho = 0.4,\ \delta = 0.15$

Similar dependences for the amplitudes of vertical oscillations are also shown here. As can be seen, for each resonance frequency there is a value at which the dissipation reaches a maximum. However, these maxima are achieved at the cost of too large amplitudes, which are unacceptable in practice for reasons of strength.

Note that the damping coefficient in this case is considered constant, whereas it can depend on the amplitude of oscillations, especially in cable-type consoles, in which the interwire friction obviously depends on the manufacturing technology. It follows that the choice of the design parameters of the damper should be based on an experimental study of its damping characteristics. The same applies to the amplitude dependence of the bending stiffness.

3. DYNAMIC STIFFNESS MATRIX OF THE DAMPER

When combining a conductor in the overhead line span with a vibration damper, it is convenient to characterize the latter with a dynamic stiffness matrix calculated at the attachment point to the clamp. Dynamic stiffness has the same meaning as static stiffness, but differs from it in that it does not relate force to displacement, but rather their amplitudes during forced vibrations, and thus depends on frequency [38].

We will proceed from equations (6), taking into account the internal damping, which now plays a significant role. We will represent the vector of amplitudes of the generalized forces acting on the clamp from the wire side in accordance with formulas (7) in the form: $\boldsymbol{Q} = \boldsymbol{Q}^0 e^{i\omega t}$. We will use a similar form for the desired solution: $\boldsymbol{q} = \boldsymbol{q}^0 e^{i\omega t}$, where $\boldsymbol{q}^0$ is the complex amplitude of the oscillations.

Let us introduce the following notation by analogy with (1.4): $\boldsymbol{Q}_0^0 = (F_C\ M_C)^T$, $\boldsymbol{0} = (0\ \ 0)^T$, $\boldsymbol{q}_i^0 = (Y_i^0\ \ \Phi_i^0)^T$, which allow us to rewrite the system (6) in expanded form:

$$-\omega^2\left(\boldsymbol{M}_{11}\boldsymbol{q}_0^0 + \boldsymbol{M}_{12}\boldsymbol{q}_1^0 + \boldsymbol{M}_{13}\boldsymbol{q}_2^0\right) = \boldsymbol{Q}_0^0,$$
$$-\omega^2\boldsymbol{M}_{12}^T\boldsymbol{q}_0^0 + \left(\boldsymbol{G}_1 - \omega^2\boldsymbol{M}_{22}\right)\boldsymbol{q}_1^0 = \boldsymbol{0},$$
$$-\omega^2\boldsymbol{M}_{13}^T\boldsymbol{q}_0^0 + \left(\boldsymbol{G}_2 - \omega^2\boldsymbol{M}_{33}\right)\boldsymbol{q}_2^0 = \boldsymbol{0}.$$

From the last two equations we express the vectors $\boldsymbol{q}_{1,2}^0$ through the vector $\boldsymbol{q}_0^0$:

$$\boldsymbol{q}_1^0 = \omega^2\left(\boldsymbol{G}_1 - \omega^2\boldsymbol{M}_{22}\right)^{-1}\boldsymbol{M}_{12}^T\boldsymbol{q}_0^0,$$
$$\boldsymbol{q}_2^0 = \omega^2\left(\boldsymbol{G}_2 - \omega^2\boldsymbol{M}_{33}\right)^{-1}\boldsymbol{M}_{13}^T\boldsymbol{q}_0^0.$$

Then from the first equation we have: $\boldsymbol{C}^*\boldsymbol{q}_0^0 = \boldsymbol{Q}_0^0$, where

$$\boldsymbol{C}^* = -\omega^2\left\{\boldsymbol{M}_{11} + \omega^2\left[\boldsymbol{M}_{12}\left(\boldsymbol{G}_1 - \omega^2\boldsymbol{M}_{22}\right)^{-1}\boldsymbol{M}_{12}^T + \right.\right.$$
$$\left.\left. + \boldsymbol{M}_{13}\left(\boldsymbol{G}_2 - \omega^2\boldsymbol{M}_{33}\right)^{-1}\boldsymbol{M}_{13}^T\right]\right\}$$

is the desired matrix of the dynamic stiffness of the damper. Note that the elements of the matrix

are complex quantities. Therefore, for example, the modulus of the displacement determined using the rigidity matrix determines its amplitude, and the argument is the phase shift of the displacement relative to the harmonic force causing it.

The obtained stiffness matrix allows to easily include the damper in the dynamic model of the span, since it can be considered as a set of concentrated "springs" characterized by dynamic stiffnesses and connected to the conductor.

CONCLUSION

The developed dynamic model covers the main properties of Stockbridge vibration dampers, widely used to reduce the amplitudes of aeolian vibration of overhead power transmission line conductors. The model and the results obtained on its basis can be used for design calculations of damper natural frequencies. The obtained dynamic stiffness can be used to include the damper in the dynamic span model, which is necessary to assess the effectiveness of the damper and determine the best position of the damper in the span.

Taking into account the nonlinearity of the elastic characteristics of the console is the subject of further development of this model.

ACKNOWLEDGEMENT

This study was carried out in accordance with the state assignment of the Institute of Applied Mechanics of the Russian Academy of Sciences.

REFERENCES

1. EPRI: Transmission Line Reference Book. Wind-Induced Conductor Motion. Electric Power Research Institute, Palo Alto, California, 1979.
2. Guidelines for standard protection against vibration and sub-vibrations of wires and lightning cables of overhead power transmission lines with a voltage of 35-750 kV. RD 34.20.182-90. Service of Excellence, ORGRES, Moscow, 1991, 70 p. (in Russian).
3. **Stockbridge G.H.** 1928. Vibration damper, U.S. Patent No. 1.675.391.
4. SALVI Research Department Paper 2. Dampers efficiency evaluation. 1968, Milan: Salvi Sp. A.
5. SALVI Research Department Paper 3. SALVI 4D damper. 1968, Milan: Salvi Sp. A.
6. **Chan J.** EPRI transmission line reference book: Wind induced-induced conductor motion. Palo Alto, California: Electric Power Research Institute, 2006.
7. **Havard D.** Assessment of the Cowal JCT x Longwood TS for vibration control. Toronto, Ontario, 2008.
8. **Claren R., Diana G.** Mathematical analysis of transmission line vibration // IEEE Transactions on Power Apparatus and Systems. 1969, PAS-88(12), pp. 1741-1771.
9. **Wagner H., Ramamurti V., Sastry R.V.R., Hartman K.** Dynamics of Stockbridge dampers // Journal of Sound and Vibration, 1973, Vol. 30(2), pp. 207-220.
10. **Allnut J.G., Rowbottom M.D.** Damping of Aeolian vibration on overhead lines by vibration dampers // Proceedings of the Institute of Electrical and Electronic Engineers, 1974, Vol. 121, pp. 1175-1178.
11. **Dhotarad M.S., Ganesan N., Rao B.V.A.** Transmission line vibration // Journal of Sound and Vibration, 1978, Vol. 60, pp. 217-227.
12. **Dhotarad M.S., Ganesan N., Rao B.V.A.** Transmission line vibration with 4R dampers // Journal of Sound and Vibration, 1978, Vol. 60, pp. 604-608.
13. **Hagedorn P**. Ein einfaches Rechenmodell zur Berechnung winderregter Schwingungen an Hochspannugsleitungen mit Dämpfern // Ingenieur Archiv, 1980, Vol. 49, ss. 161-177.

14. **Hagedorn P.** On the optimal design of Stockbridge dampers // Proceedings of CIGRE Symposium, Stockholm, 1981, S 22-81, paper 112-10.
15. **Schäfer B.** The energy method and the exact solution for conductor oscillations, a comparison // Proceedings of CIGRE Symposium, Stockholm, 1981, S 22-81, paper 112-11.
16. **Markiewicz M.** Optimum dynamic characteristics of Stockbridge dampers for dead-end spans // Journal of Sound and Vibration, 1995, Vol. 188(2), pp. 243-256.
17. **Sauter D., Hagedorn P.** On the hysteresis of wire cables in Stockbridge dampers // International Journal of Non-linear Mechanics, 2002, Vol. 37, pp. 1435-1459.
18. **Lu M.L., Chan J.K.** An efficient algorithm for Aeolian vibration of single conductor with multiple dampers // IEEE Transactions on Power Delivery, 2007, Vol. 22(3), pp. 1822-1829.
19. **Barbieri N., Barbieri R.** Dynamic analysis of Stockbridge damper // Advances in Acoustics and Vibration, 2012, Article ID 659398, 8 p.
20. **Li L., Cao H., Jiang Y., Chen Y.,** Experimental study on mitigation devices of Aeolian vibration of bundled conductors // Journal of Vibration and Control, 2013, Vol. 22, pp. 1217-1227.
21. **Langlois S., Legeron F.** Prediction of Aeolian vibration of transmission line conductors using a nonlinear time history model – Part I: Damper model // IEEE Transactions of Power Delivery, 2014, Vol. 29, Iss. 3, pp. 1168-1175.
22. **Langlois S., Legeron F.** Prediction of Aeolian vibration of transmission line conductors using a nonlinear time history model – Part II: Conductor and damper model // IEEE Transactions of Power Delivery, 2014, Vol. 29, Iss. 3, pp. 1176-1183.
23. **Barry O., Zu J.W., Oguamanam D.C.D.** Nonlinear dynamics of Stockbridge dampers // Journal of Dynamic Systems. Measurement and Control, 2015, Vol. 137, pp. 1-7.
24. **Barbieri N., Barbieri R., Silva R.A., Mannala M.J., Barbieri L.S.** Nonlinear dynamic analysis of wire-rope isolator and Stockbridge damper // Nonlinear Dynamics, 2016, Vol. 86, pp. 501-512.
25. **Havard D.** Interaction of vibration dampers with surge arresters CIGRÉ B2 TF 007. Convenor CIGRE Science & Engineering, 2016, Vol. 6, pp. 32-45.
26. **Vaja N., Barry O., Tanbour E.** On the modeling and analysis of a vibration absorber for overhead powerlines with multiple resonant frequencies // Engineering Structures, 2018, Vol. 175, pp. 711-720.
27. **Foti F., Martinelli L.** Hysteretic behavior of Stockbridge dampers: modelling and parameter identification // Mathematical Problems in Engineering, 2018, Vol. 2018, Article ID 8925121, 17 p.
28. **Luo X., Wang L., Zhang Y.** Nonlinear numerical model with contact for Stockbridge vibration damper and experimental validation // Journal of Vibration and Control, 2016, Vol. 22(5), pp. 1217-1227.
29. **Luo X.Y., Zhang Y.S., Zheng Y.P.** Nonlinear revision of the linear model for Stockbridge vibration damper and experiment validation // Applied Mechanics and Materials, 2013, Vol. 328, pp. 504-508.
30. **Panovko Ya.G.** Internal friction during vibrations of elastic systems. Moscow, Fizmatgiz, 1960, 193 p. (in Russian).
31. **Sorokin E.S.** On the theory of internal friction during vibrations of elastic systems. Moscow, Gosstroizdat, 1960, 131 p. (in Russian).
32. **Papailiou K.O.** On the bending stiffness of transmission line conductors // IEEE Transactions on Power Delivery, 1997, Vol. 12(4), pp. 1576-1588.
33. Recommendations for the use of multi-frequency vibration dampers of GWP and unified vibration dampers of GWP on overhead transmission lines with a voltage of 35-750 kV. FROM 34.20.264-2005. Mos-

cow: Center for industrial and technical information of energy enterprises and technical training ORGRES. 2008. 20 p. (in Russian).
34. **Filippov A.P.** Vibrations of elastic systems. Kiev, Ed. Academy of Sciences of the Ukrainian SSR, 1956, 322 p. (in Russian).
35. **Loitsyansky L.G., Lurie A.I.** Course of theoretical mechanics. Vol. II, Moscow, Nauka, 1983, 640 p. (in Russian).
36. GOST R 51155-2017. Linear fittings. Acceptance rules and test methods, Moscow, Standartinform, 2017, 42 p. (in Russian).
37. **Den Hartog J.P.** Mechanical vibrations. Dover Publications, Inc., N.Y., 1985, 449 p.
38. **Panovko Ya.G., Gubanova I.I.** Stability and oscillations of elastic systems. Moscow, Nauka, 1964, 336 p. (in Russian).

СПИСОК ЛИТЕРАТУРЫ

1. EPRI: Transmission Line Reference Book. Wind-Induced Conductor Motion. Electric Power Research Institute, Palo Alto, California, 1979.
2. Методические указания по типовой защите от вибрации и субколебаний проводов и грозотросов воздушных линий электропередачи напряжением 35-750 кВ. РД 34.20.182-90. Служба передового опыта, ОРГРЭС: М., 1991, 70 с.
3. **Stockbridge G.H.** 1928. Vibration damper, U.S. Patent No. 1.675.391.
4. SALVI Research Department Paper 2. Dampers efficiency evaluation. 1968, Milan: Salvi Sp. A.
5. SALVI Research Department Paper 3. SALVI 4D damper. 1968, Milan: Salvi Sp. A.
6. **Chan J.** EPRI transmission line reference book: Wind induced-induced conductor motion. Palo Alto, California: Electric Power Research Institute, 2006.
7. **Havard D.** Assessment of the Cowal JCT x Longwood TS for vibration control. Toronto, Ontario, 2008.
8. **Claren R., Diana G.** Mathematical analysis of transmission line vibration // IEEE Transactions on Power Apparatus and Systems. 1969, PAS-88(12), pp. 1741-1771.
9. **Wagner H., Ramamurti V., Sastry R.V.R., Hartman K.** Dynamics of Stockbridge dampers // Journal of Sound and Vibration, 1973, Vol. 30(2), pp. 207-220.
10. **Allnut J.G., Rowbottom M.D.** Damping of Aeolian vibration on overhead lines by vibration dampers // Proceedings of the Institute of Electrical and Electronic Engineers, 1974, Vol. 121, pp. 1175-1178.
11. **Dhotarad M.S., Ganesan N., Rao B.V.A.** Transmission line vibration // Journal of Sound and Vibration, 1978, Vol. 60, pp. 217-227.
12. **Dhotarad M.S., Ganesan N., Rao B.V.A.** Transmission line vibration with 4R dampers // Journal of Sound and Vibration, 1978, Vol. 60, pp. 604-608.
13. **Hagedorn P**. Ein einfaches Rechenmodell zur Berechnung winderregter Schwingungen an Hochspannugsleitungen mit Dämpfern // Ingenieur Archiv, 1980, Vol. 49, ss. 161-177.
14. **Hagedorn P.** On the optimal design of Stockbridge dampers // Proceedings of CIGRE Symposium, Stockholm, 1981, S 22-81, paper 112-10.
15. **Schäfer B.** The energy method and the exact solution for conductor oscillations, a comparison // Proceedings of CIGRE Symposium, Stockholm, 1981, S 22-81, paper 112-11.
16. **Markiewicz M.** Optimum dynamic characteristics of Stockbridge dampers for dead-end spans // Journal of Sound and Vibration, 1995, Vol. 188(2), pp. 243-256.
17. **Sauter D., Hagedorn P.** On the hysteresis of wire cables in Stockbridge dampers // International Journal of Non-linear Mechanics, 2002, Vol. 37, pp. 1435-1459.
18. **Lu M.L., Chan J.K.** An efficient algorithm for Aeolian vibration of single conductor with multiple dampers // IEEE Transactions

on Power Delivery, 2007, Vol. 22(3), pp. 1822-1829.
19. **Barbieri N., Barbieri R.** Dynamic analysis of Stockbridge damper // Advances in Acoustics and Vibration, 2012, Article ID 659398, 8 p.
20. **Li L., Cao H., Jiang Y., Chen Y.,** Experimental study on mitigation devices of Aeolian vibration of bundled conductors // Journal of Vibration and Control, 2013, Vol. 22, pp. 1217-1227.
21. **Langlois S., Legeron F.** Prediction of Aeolian vibration of transmission line conductors using a nonlinear time history model – Part I: Damper model // IEEE Transactions of Power Delivery, 2014, Vol. 29, Iss. 3, pp. 1168-1175.
22. **Langlois S., Legeron F.** Prediction of Aeolian vibration of transmission line conductors using a nonlinear time history model – Part II: Conductor and damper model // IEEE Transactions of Power Delivery, 2014, Vol. 29, Iss. 3, pp. 1176-1183.
23. **Barry O., Zu J.W., Oguamanam D.C.D.** Nonlinear dynamics of Stockbridge dampers // Journal of Dynamic Systems. Measurement and Control, 2015, Vol. 137, pp. 1-7.
24. **Barbieri N., Barbieri R., Silva R.A., Mannala M.J., Barbieri L.S.** Nonlinear dynamic analysis of wire-rope isolator and Stockbridge damper // Nonlinear Dynamics, 2016, Vol. 86, pp. 501-512.
25. **Havard D.** Interaction of vibration dampers with surge arresters CIGRÉ B2 TF 007. Convenor CIGRE Science & Engineering, 2016, Vol. 6, pp. 32-45.
26. **Vaja N., Barry O., Tanbour E.** On the modeling and analysis of a vibration absorber for overhead powerlines with multiple resonant frequencies // Engineering Structures, 2018, Vol. 175, pp. 711-720.
27. **Foti F., Martinelli L.** Hysteretic behavior of Stockbridge dampers: modelling and parameter identification // Mathematical Problems in Engineering, 2018, Vol. 2018, Article ID 8925121, 17 p.
28. **Luo X., Wang L., Zhang Y.** Nonlinear numerical model with contact for Stockbridge vibration damper and experimental validation // Journal of Vibration and Control, 2016, Vol. 22(5), pp. 1217-1227.
29. **Luo X.Y., Zhang Y.S., Zheng Y.P.** Nonlinear revision of the linear model for Stockbridge vibration damper and experiment validation // Applied Mechanics and Materials, 2013, Vol. 328, pp. 504-508.
30. **Пановко Я.Г.** Внутреннее трение при колебаниях упругих систем. М.: Физматгиз. 1960. 193 с.
31. **Сорокин Е.С.** К теории внутреннего трения при колебаниях упругих систем. М.: Госстройиздат. 1960. 131 с.
32. **Papailiou K.O.** On the bending stiffness of transmission line conductors // IEEE Transactions on Power Delivery, 1997, Vol. 12(4), pp. 1576-1588.
33. Рекомендации по применению многочастотных гасителей вибрации ГВП и унифицированных гасителей вибрации ГВУ на воздушных линиях электропередачи напряжением 35-750 кВ. СО 34.20.264-2005. М.: Центр производственно-технической информации энергопредприятий и технического обучения ОРГРЭС. 2008. 20 с.
34. **Филиппов А.П.** Колебания упругих систем. Киев: Изд. АН УССР, 1956. 322 с.
35. **Лойцянский Л.Г., Лурье А.И.** Курс теоретической механики. Т. II. М.: Наука. 1983. 640 с.
36. ГОСТ Р 51155-2017. Арматура линейная. Правила приемки и методы испытаний. М., Стандартинформ, 2017. 42 с.
37. **Ден-Гартог Д.П.** Механические колебания. М., Физматгиз, 1960, 580 с.
38. **Пановко Я.Г., Губанова И.И.** Устойчивость и колебаний упругих систем. М., Наука, 1964, 336 с.

Alexander Nikolaevich Danilin, Doctor of Physical and Mathematical Sciences, Chief Researcher, Institute of Applied Mechanics of the Russian Academy of Sciences (IAM RAS); Department of Mechanics of Adaptive Composite Materials and Systems; 7, building 1, Leningradsky Prospekt, Moscow, 125040, Russia; andanilin@yandex.ru;

Andrey Petrovich Zakharov, postgraduate student, IAM RAS; Department of Mechanics of Adaptive Composite Materials and Systems; 7, building 1, Leningradsky Prospekt, Moscow, 125040, Russia; andreyzakharoff@yandex.ru

Alexander Evgenievich Fedorov, postgraduate student, IAM RAS; Department of Mechanics of Adaptive Composite Materials and Systems; 7, building 1, Leningradsky Prospekt, Moscow, 125040, Russia; iam@iam.ras.ru

Valery Adolfovich Feldstein, Doctor of Technical Sciences, Leading Researcher, IAM RAS; Department of Mechanics of Adaptive Composite Materials and Systems; 7, building 1, Leningradsky Prospekt, Moscow, 125040, Russia; dinpro@mail.ru

Александр Николаевич Данилин, доктор физико-математических наук, главный научный сотрудник ФГБУН Института прикладной механики Российской академии наук (ИПРИМ РАН); Отдел механики адаптивных композиционных материалов и систем; д.7, стр.1, Ленинградский просп., Москва, 125040, Россия; andanilin@yandex.ru;

Андрей Петрович Захаров, аспирант ИПРИМ РАН; Отдел механики адаптивных композиционных материалов и систем; д.7, стр.1, Ленинградский просп., Москва, 125040, Россия; andreyzakharoff@yandex.ru

Александр Евгеньевич Фёдоров, аспирант ИПРИМ РАН; Отдел механики адаптивных композиционных материалов и систем; д.7, стр.1, Ленинградский просп., Москва, 125040, Россия; iam@iam.ras.ru

Валерий Адольфович Фельдштейн, доктор технических наук, ведущий научный сотрудник ИПРИМ РАН; Отдел механики адаптивных композиционных материалов и систем; д.7, стр.1, Ленинградский просп., Москва, 125040, Россия; dinpro@mail.ru